Catal Lett (2015) 145:1022–1032
DOI 10.1007/s10562-015-1498-3

New Vanadium Keggin Heteropolyacids Encapsulated in a Silica Framework: Recyclable Catalysts for the Synthesis of Highly Substituted Hexahydropyrimidines Under Suitable Conditions

Valeria Palermo · Ángel Sathicq · Thierry Constantieux · Jean Rodríguez · Patricia Vázquez · Gustavo Romanelli

Received: 8 January 2015 / Accepted: 5 February 2015 / Published online: 19 February 2015

Abstract Solid acid catalysts based on the direct incorporation of the vanadium Keggin heteropolyacid (PMo11V) structure during the synthesis of silica by the sol–gel technique, in acidic media using tetraethyl orthosilicate ($PMo11VSiO_2$1, $PMo11VSiO_2$2, $PMo11VSiO_2$3, and $PMo11VSiO_2$4), were prepared and characterized by ^{31}P-NMR, FT-IR, XRD, and textural properties (S_{BET}). The acidic characteristics of the catalysts were determined by potentiometric titration with *n*-butylamine. A series of highly substituted hexahydropyrimidines were synthesized using these new materials, encapsulated in a silica framework, as catalyst in solvent-free conditions. This methodology requires short reaction time (1.5 h), a temperature of 80 °C in solvent free-conditions to obtain good to excellent yields of trifluoromethyl-hexahydropyrimidine derivatives. The Keggin catalyst embedded in the silica matrix is insoluble in polar media, which allows easy removal of the reaction products without affecting their catalytic activity.
Graphical Abstract

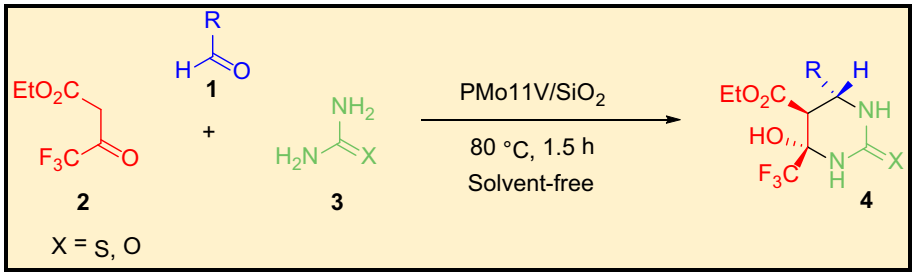

V. Palermo · Á. Sathicq · P. Vázquez · G. Romanelli (✉)
Centro de Investigación y Desarrollo en Ciencias Aplicadas 'Dr. Jorge J. Ronco' (CINDECA-CCT-CONICET), Universidad Nacional de La Plata, Calle 47 No. 257, B1900AJK La Plata, Argentina
e-mail: gpr@quimica.unlp.edu.ar

T. Constantieux · J. Rodríguez
Institut des Sciences Moléculaires de Marseille-UMR CNRS 7313 iSm2, Aix-Marseille Université Centre Saint Jérôme, Service 531, 13397 Marseille Cedex 20, France

G. Romanelli
Cátedra de Química Orgánica, Facultad de Ciencias Agrarias y Forestales, CISAV, Universidad Nacional de La Plata, Calles 60 y 119 s/n, B1904AAN La Plata, Argentina

Keywords Keggin heteropolyacids · Silica sol–gel · HPA included in silica matrix · Trifluoromethyl-hexahydropyrimidines · Multicomponent reaction

1 Introduction

The utilization of heterogeneous catalysts has gained much interest in recent decades due to economic and environmental considerations. These heterogeneous catalysts are more advantageous over homogeneous catalysts, mainly because they can be easily recovered from the reaction mixture by simple filtration procedures and then reused

after activation, thereby making the process economically viable [1–3].

The need for greener procedures leads to the utilization of different environmentally friendly reaction conditions; among them, the elimination of volatile organic solvents in organic syntheses is the most important goal in 'green' chemistry [4, 5]. Solvent-free organic reactions make syntheses simpler, save energy, and prevent hazardous solvent waste and toxicity. The development of solvent-free organic reaction has thus become an important research area, and a large number of papers on these reactions, which include the reaction between solids, solids and liquid, liquids and, on solid supports, have become increasingly frequent in recent years [6].

Also, the replacement of toxic inorganic acid catalysts such as sulfuric, fluorhydric or hydrochloric acids with reusable solid acids and the use of room temperature avoiding media heating are still necessary. In recent years, inorganic, organic and hybrid solid materials, catalyzed organic transformations, due to the proven simplified product isolation, mild reaction conditions, high selectivity, easy recovery, and catalyst reuse and reduction in by-product generation [7–9].

Catalysis by heteropolyacids (HPAs) is a field of increasing importance worldwide. Numerous developments are being carried out in research as well as in chemistry processes [10].

On the other hand, HPAs possess a very strong acidity and appropriate redox properties, which can be changed by varying the chemical composition of the heteropolyanion. The reactions catalyzed by HPAs have been reviewed by many researchers [11–13]. As part of a research project to develop environmentally friendly organic reactions, we used different bulk and silica-supported Keggin, Wells–Dawson and Preyssler heteropolyacids in the preparation of nitrogenated heterocyclic synthesis, under greener conditions, such as the synthesis of 3,4-dihydropyrimidin-2(1H)-(thio)ones [14], 1,4-dihydropyridines [15], 4-arylidene-2-phenyl-5(4)-oxazolones [16], N-sulfonyl-1,2,3,4-tetrahydroisoquinolines [17], quinoxalines [18], and 1,5-benzodiazepines [19].

Organic catalytic transformations using HPAs as solid acid catalysts have many advantages; for example, they are noncorrosive, cheap and environmentally friendly, presenting fewer disposal problems. However, their solubility in polar solvents and the low specific area of bulk HPAs limit their use as heterogeneous catalysts. So attempts to stabilize HPAs by supporting them on several carriers such as silica, alumina, titania, among others, have been made [20]. However, the supported HPA catalysts obtained by impregnation techniques are unsuitable for their use as catalysts in polar reaction media due to a continuous leaching of the HPAs. In order to avoid any HPA leaching, some papers have reported the inclusion of the HPAs in silica using a sol–gel technique by the hydrolysis of ethyl orthosilicate [21–23].

On the other hand, heterocyclic compounds bearing pyrimidines are an important family of substances that play a key role in organic synthesis, because they are present in a variety of naturally occurring or synthetic compounds. Particularly, both natural and synthetic molecules containing pyrimidine moiety have interesting pharmacological and biological properties [24]. Among all heterocyclic compounds, pyrimidines are one of the most important heterocycles exhibiting remarkable pharmacological activities because they are an essential constituent of all cells and thus of all living matter [24, 25].

Particularly, hexahydropyrimidines are biologically important, for example, bisalkylhexahydropyrimidines are effective against Ehrlich carcinoma and Staphylococcus aureus [26]. Also, the hexahydropyrimidine skeleton occurs in alkaloids such as tetraponerines, verbametrine and verbamethine, which are synthetic intermediates for spermidine-nitroimidazole drugs, and is used for the treatment of A549 lung carcinoma [26]. Benzo-fused hexahydropyrimidines possess antiplatelet activity [27] and are potential R-adrenergic blockers [28].

Hexahydropyrimidines are prepared generally by condensations of aldehydes and ketones with substituted 1,3-diaminopropanes [29, 30]. In 1999 O. Kappe and coworkers discovered that by using a fluorinated acetoacetic ester derivative, for example, ethyl trifluoroacetate, the Biginelli reaction, used to obtain 3,4-dihydro-2(1*H*)-pyrimidinones, takes a different course and trifluoromethylated hexahydropyrimidines are obtained in excellent yields [31].

The preparation methods for the synthesis of these compounds include the multicomponent reaction of an aldehyde, 1,3-dicarbonyl compounds and urea or thiourea, in the presence of different catalysts, including (HCl [32], *p*-toluenesulfonic acid [33], sulfamic acid [34], benzyltriethylammonium chloride [35], chlorotrimethylsilane [36], zirconium (IV) chloride [37]), and Preyssler heteropolyacid included in silica matrix [38].

The present protocol allows the introduction of fluorine atoms in the hexahydropyrimidine structures, during the multicomponent synthesis, in one step, representing a powerful alternative for the design of new drugs. A fluorine atom is similar in size to a hydrogen atom. Thus, the replacement of hydrogen by fluorine does not cause any changes in molecular geometry. The elevated electronegativity of fluorine has a strong effect on the electronic properties of the molecules. On a molecular level, this allows for the inhibition of some metabolic pathways, including the modulation of membrane permeability, as well as electrostatic interactions with the target site [39].

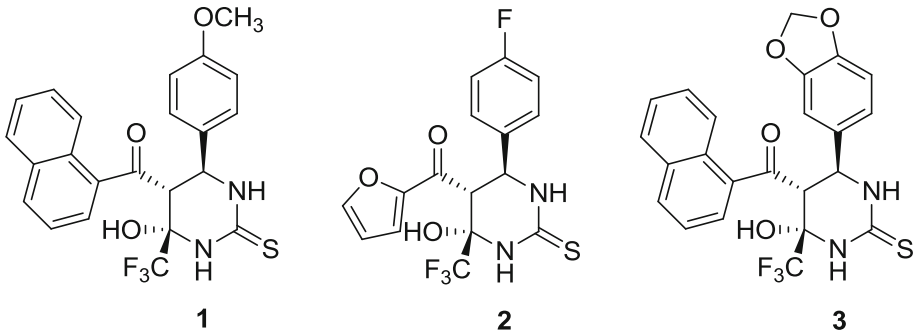

Fig. 1 Promising new leads for the development of highly potent and selective anticancer compounds

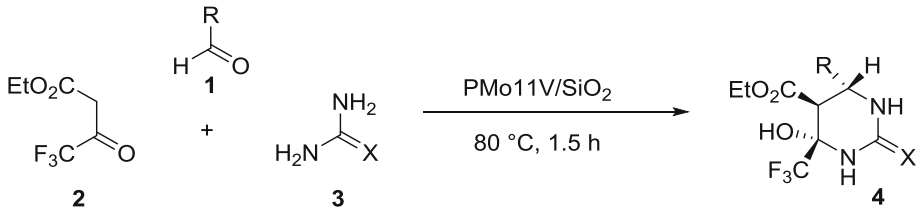

Scheme 1 Synthesis of fluorinated hexahydropyrimidine

Trifluoromethylated hexahydropyrimidine derivatives (compounds 1, 2, and 3 in Fig. 1) represent promising new leads for the development of highly potent and selective anticancer compounds [40].

In the present paper, we report the synthesis and characterization of four materials obtained by direct incorporation of different amounts of a heteropolyacid with Keggin structure (PMo11V) during the synthesis of silica by the sol–gel technique, in acidic media, using tetraethyl orthosilicate. The catalyst characterization was carried out by ^{31}P MAS-NMR, FT-IR, XRD, textural properties (S_{BET}), and the acidic properties were determined through potentiometric titration with *n*-butylamine.

In addition, we studied the application of these recyclable solid catalysts in a simple, convenient, efficient, and ecofriendly process for the multicomponent preparation of trifluoromethylated hexahydropyrimidines from aldehydes, trifluoromethylacetoacetate and urea or thiourea under solvent-free conditions (Scheme 1).

2 Experimental

2.1 Catalytic Synthesis

2.1.1 Bulk Heteropolyacid Synthesis

$H_3PMo_{12}O_{40}$ (PMo12) is a commercial product (Fluka) and was used without further purification. $H_4PMo_{11}VO_{40}$ (PMo11V) was prepared by a hydrothermal synthesis method, following a procedure described in the literature [41]. A stoichiometric mixture of 0.58 mL of (85 % (w/V)) phosphoric acid, 0.91 g of vanadium pentoxide, and 14.4 g of molybdenum trioxide was suspended in 150 mL of distilled water. The mixture was stirred at 80 °C for 3 h. After cooling down to room temperature and removal of insoluble molybdates and vanadates, the heteropolyacid solution was evaporated and dried at 85 °C, for 24 h. After that, orange crystals of PMo11V were obtained.

2.1.2 Synthesis of Silica-Included PMo12 and PMo11V

A series of PMo12 and PMo11V immobilized on silica with different HPA loadings were prepared. The catalytic agent samples were prepared according to Caetano et al. [21], by the sol–gel technique. A mixture of water (1.0 mol), ethanol (0.1 mol), and a variable amount of heteropolyacids (from 1.25×10^{-4} to 5.00×10^{-4} mol) was added to tetraethyl orthosilicate (0.1 mol), and stirred at 80 °C for 3 h. The hydrogel obtained was dehydrated slowly at 80 °C, for 1.5 h, in vacuo. The dried gel obtained was washed three times with reflux ethanol and dried at 100 °C overnight. The prepared catalysts were named as $PMo11VSiO_2$1, $PMo11VSiO_2$2, $PMo11VSiO_2$3, $PMo11VSiO_2$4, and $PMo12SiO_2$3.

2.2 Catalyst Characterization

2.2.1 Inductively Coupled Plasma Atomic Emission Spectroscopy

The experimental contents of Mo, V in the bulk HPA were determined by means of the inductively coupled plasma atomic emission spectroscopy (ICP-AES) technique using a Shimadzu 1000 III instrument.

2.2.2 Textural Properties

The specific surface area of the solids was determined from the N_2 adsorption–desorption isotherms at liquid-nitrogen temperature. They were obtained using Micromeritics ASAP 2020 equipment. The samples were previously degassed at 100 °C for 12 h. The specific surface area (S_{BET}) was determined by the BET method.

2.2.3 Fourier Transform Infrared Spectroscopy

FT-IR spectra of the support and catalysts were obtained in the 400–4000 cm^{-1} wavenumber range using pellets of KBr in a Thermo Bruker IFS 66 FT-IR spectrometer.

2.2.4 X-ray Diffraction

The XRD patterns were collected in Philips PW-1730 equipment. The X-ray source was Cu Kα radiation ($\lambda = 1.5406$ Å) with 40 kV and 20 mA. Nickel filter and scanning angle between 5 and 60° of 2θ at a scanning rate of 2° per minute were used.

2.2.5 ^{31}P-NMR Spectra

The ^{31}P magic angle spinning-nuclear magnetic resonance (^{31}P MAS-NMR) spectra were recorded with Bruker 9.4 T Avance III WB 400 equipment, working at a frequency of 161.9 MHz for ^{31}P. The spin rate was 35 kHz and several hundred pulse responses were collected.

2.2.6 Potentiometric Titration

A suspension of the solid (25 mg), in acetonitrile, was titrated using 0.025 N *n*-butylamine in acetonitrile, at a flow rate 0.05 mL/min in 794 Basic Titrino Metrohm equipment using a double junction electrode.

The acidic properties of the samples measured by this technique enable the evaluation of the total number of acid sites and their acid strength. In order to interpret the results, it is suggested that the initial electrode potential (E) indicates the maximum acid strength of the surface sites, and the values (meq/g solid), where the plateau is reached, indicate the total number of acid sites. The acid strength of surface sites can be assigned according to the following ranges: very strong site, $E > 100$ mV; strong site, $0 < E < 100$ mV; weak site, $-100 < E < 0$ mV, and very weak site, $E < -100$ mV [42].

2.3 Catalytic Activity Test

2.3.1 General

Chemicals were purchased from Aldrich, Fluka and Merck and were freshly used after purification by standard procedures (distillation and recrystallization). All the reactions were monitored by TLC on pre-coated silica gel plates (254 mm). All the products were identified by comparison of physical data (mp, TLC and NMR) with those reported or with those of authentic samples prepared by the respective conventional methods using sulfuric acid as catalyst. Melting points of the compounds were determined in sealed capillary tubes and are uncorrected. The ^{1}H-NMR and ^{13}C-NMR spectra were obtained on a Bruker instrument 400 MHz model as $CDCl_3$ solutions, and the chemical shifts were expressed in d units with Me4Si (TMS) as the internal standard.

2.3.2 General Procedure for the Synthesis of Hexahydropyrimidines

The reaction was performed in a round bottom flask, which was equipped with a condenser and immersed in an oil bath. A mixture of ethyltrifluoroacetoacetate (184 mg, 1 mmol), benzaldehyde (281 mg, 1 mmol), urea (72 mg, 1.2 mmol), and the selected catalyst was thoroughly mixed, and then heated at 80 °C for 1.5 h (to end point of the reaction, checked by TLC). On cooling, the reaction mixture was washed with acetone (2 × 1 mL), and the hexahydropyrimidines were filtered and dried under vacuum (25 °C). The crude product was recrystallized to give the pure dihydropyrimidinones.

2.3.3 Catalyst Reuse

Stability tests of the bulk or silica-supported acid catalysts were carried out running four consecutive experiments, under the same reaction conditions. After each test, the catalyst was separated from the reaction mixture by filtration, washed with acetone (2 × 2 mL), dried under vacuum, and then reused.

Table 1 Elemental analysis by ICP-AES

HPA	Theoretical value	Experimental value (ICP-AES)
PMo12	Mo 55.98	Mo 50.70
PMo11V	Mo 52.36	Mo 52.85
	V 2.53	V 3.4

3 Results and Discussion

3.1 Catalyst Characterization

3.1.1 Inductively Coupled Plasma Atomic Emission Spectroscopy

The elemental analysis by ICP-AES of the bulk HPA is shown in Table 1. The experimental values are in agreement with the theoretical values for the hydrated PMo12 and PMo11V ($H_3PMo_{12}O_{40}\cdot 13H_2O$ and $H_4PMo_{11}VO_{40}\cdot 13H_2O$). For the synthesized vanadium HPA, this technique confirms that one of the Mo atoms was replaced by one V atom.

3.1.2 Textural Properties

The adsorption–desorption isotherms of the silica-included HPA and the silica support are typical of microporous materials. As example, Fig. 2 shows the isotherms of $PMo12SiO_23$, $PMo11VSiO_23$, and SiO_2. Table 2 lists the specific area values, determined using the BET method (S_{BET}), the pore volume and pore size distribution for the silica and silica-included HPA. It was observed that the S_{BET} values of the silica-included HPA are in the order of the specific area of pure silica and increase with the HPA loading.

Comparing the silica-included with the same load but different HPA ($PMo11VSiO_23$ and $PMo12SiO_23$) it can be seen that the superficial area, pore volume and size distribution are in the same order of the pure silica. When the load of HPA are 5.07 and 9.03 wt% ($PMo11VSiO_21$ and $PMo11VSiO_22$) the superficial area and pore volume is lower than the pure silica, possibly due the pore blocking for the HPA remaining inside the silica structure.

On the other hand, when a higher amount of HPA ($PMo11VSiO_23$ and $PMo11VSiO_24$) is used, the excess of the HPA could interfere during the ageing process, preventing strong compression of the silica framework, with the slight increment in the pore volume and superficial area.

3.1.3 Fourier Transform Infrared Spectroscopy

The FT-IR spectra of silica-included HPA show the characteristic peaks of pure silica, without any significant

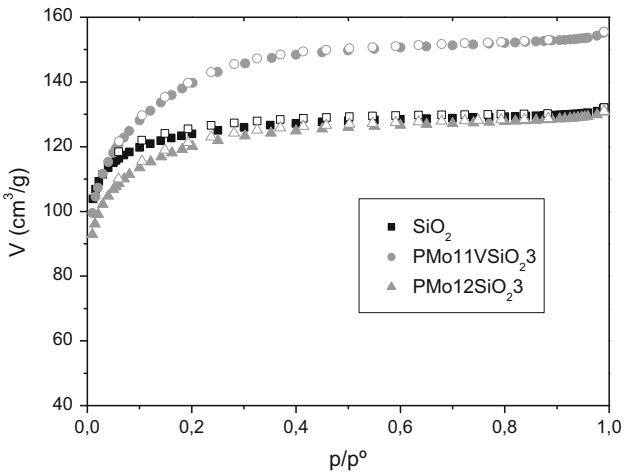

Fig. 2 N_2 (*filled circle*) adsorption- (*empty circle*) desorption isotherms for $PMo12SiO_23$, $PMo11VSiO_23$, and silica

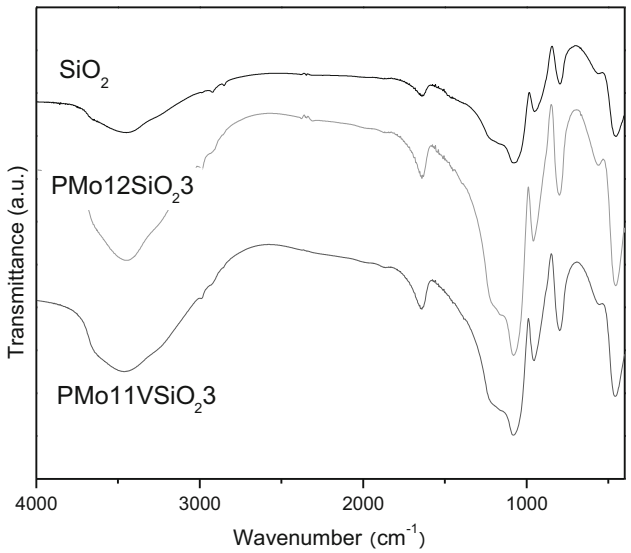

Fig. 3 FT-IR spectra of $PMo11VSiO_23$, $PMo12SiO_23$, and SiO_2

Table 2 HPA/silica ratio, specific area (S_{BET}), pore volume, pore size distribution and acid strength of silica-included HPA

Catalyst	HPA/silica (wt%)[a]	S_{BET} (m^2/g)	Pore volume (cm^3/g)	Pore Size distribution (Å)	E (mV)
SiO_2	–	438	0.20	18.6	33
$PMo11VSiO_21$	5.07	372	0.17	18.8	80
$PMo11VSiO_22$	9.03	289	0.14	18.7	279
$PMo11VSiO_23$	10.92	495	0.24	19.4	413
$PMo11VSiO_24$	17.69	547	0.27	19.9	443
$PMo12SiO_23$	11.73	425	0.20	19.0	316

[a] Respect the initial load

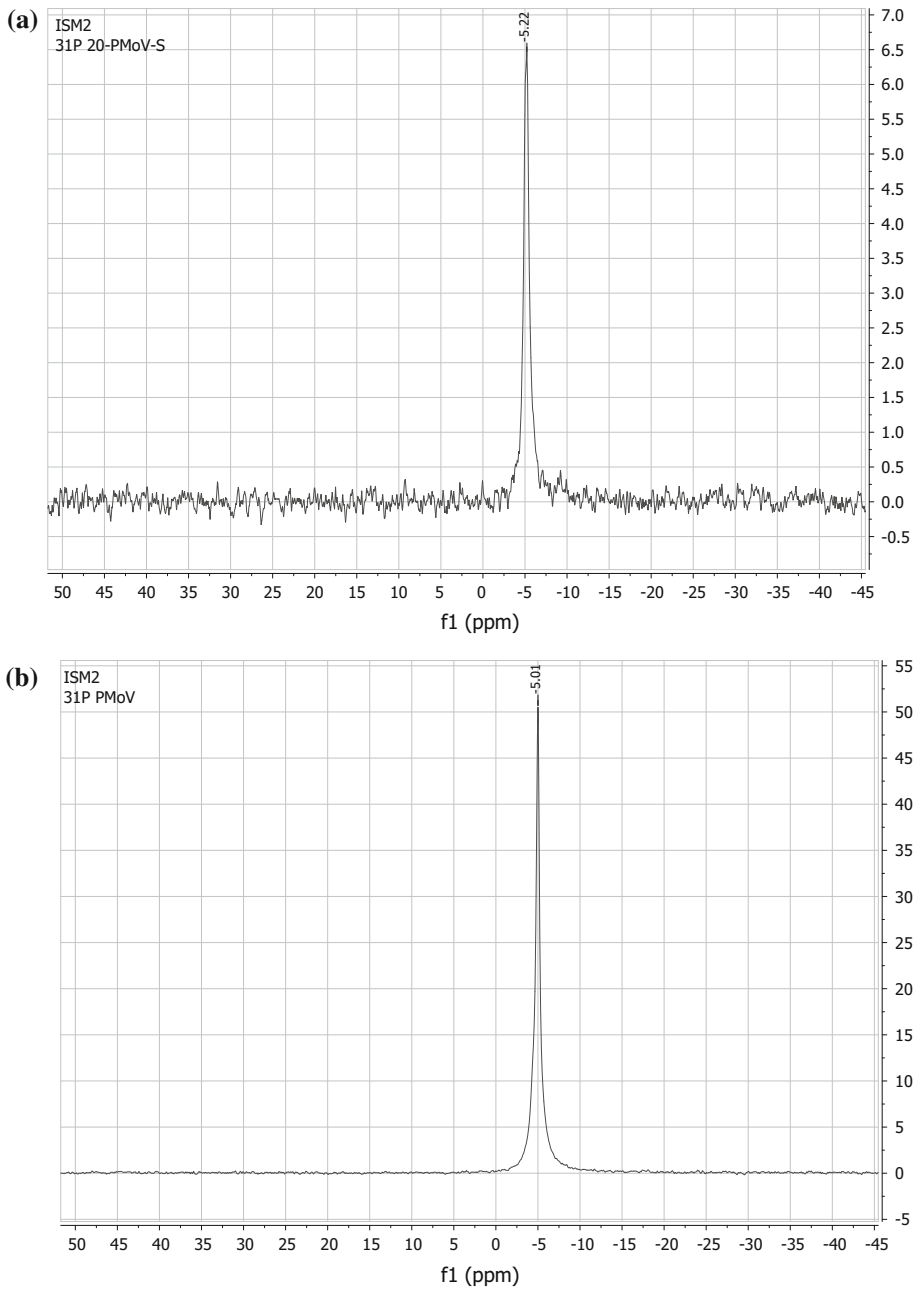

Fig. 4 ^{31}P-MAS-NMR spectra of, **a** PMo11VSiO$_2$2 and **b** PMo11V

differences with respect to the HPA or the loading amount. Figure 3 shows the FT-IR spectra of silica-included HPA catalysts PMo11VSiO$_2$3, PMo12SiO$_2$3, and SiO$_2$. The most intense band, at 1080 cm^{-1}, is associated with the O–Si–O stretching vibration, a shoulder at 1196 cm^{-1} is due to shape effects of the stretching and bending modes; the other O–Si–O bands are 797 cm^{-1} (flection) and 453 cm^{-1} (balance). The peak at 951 cm^{-1} is associated with Si–OH stretching, while the band at 1639 cm^{-1} corresponds to the SiO–H bending mode and the broad band at 3500 cm^{-1} corresponds to O–H stretching [43]. The typical bands of the Keggin structure of PMo12 (1064 cm^{-1} (P-Oa), 962 (Mo-Od) cm^{-1}, 871 cm^{-1} (Mo-Ob-Mo), 780 cm^{-1} (Mo-Oc-Mo)), and PMo11 V (1060 cm^{-1} (P-Oa), 960 cm^{-1} (M-Od), 864 cm^{-1} (M-Ob-M), 777 cm^{-1} (M-Ob-M)) are masked by the silica bands (O_a surrounds the central tetrahedral P, and links P and M together; O_b connects MO_6 octahedra by the corners; O_c shares the octahedra edges; and terminal oxygen O_d is bonded to only one M atom.).

3.1.4 X-ray Diffraction

The XRD patterns (not shown) of silica-included HPA present the same pattern as amorphous pure silica. In the former, the characteristic peaks of PMo12 and PMo11V are

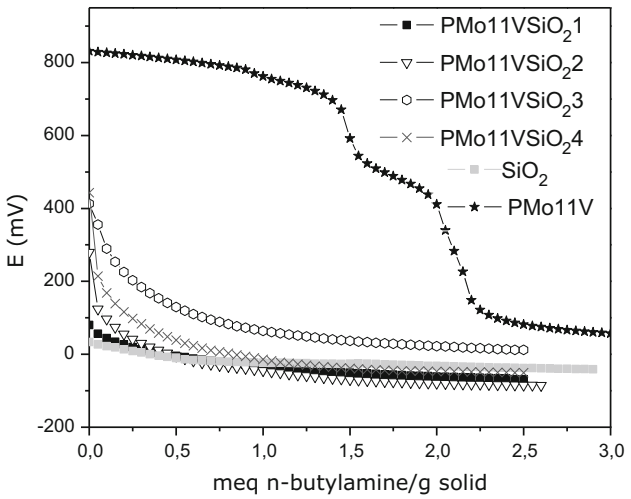

Fig. 5 Potentiometric titration of PMo11V catalysts

Table 3 Effect of different catalysts on fluorinated hexahydropyrimidine yields (%)

Entry	Catalyst	Yields (%)[a]
1	None	<5
2	SiO_2	16
3	PMo12	48
4	PMo11V	55
5	PMo12$SiO_2$3	70
6	PMo11V$SiO_2$1	81
7	PMo11V$SiO_2$2	82
8	PMo11V$SiO_2$3	84
9	PMo11V$SiO_2$4	86

Reaction conditions: benzaldehyde (281 mg, 1 mmol); ethyltrifluoroacetoacetate (184 mg, 1 mmol); urea (72 mg, 1.2 mmol); catalyst (5 mg); temperature, 80 °C; time, 1.5 h; stirring; in solvent-free conditions

[a] The crude product was recrystallized

Table 4 Effect of temperature on fluorinated hexahydropyrimidine yield (%)

Entry	Temperature (°C)	Yield (%)[a]
1	25	15
2	60	70
3	80	85
4	100	80

Reaction conditions: benzaldehyde (281 mg, 1 mmol); ethyltrifluoroacetoacetate (184 mg, 1 mmol); urea (72 mg, 1.2 mmol); PMo11V$SiO_2$1 (10 mg); time, 1.5 h; stirring; in solvent-free conditions

[a] The crude product was recrystallized

not present. According to the FT-IR spectra, the diffraction patterns show a high dispersion of HPA into the silica framework.

Table 5 Effect of reaction time on fluorinated hexahydropyrimidine yields (%)

Entry	Reaction time (h)	Yield (%)[a]
1	0.5	64
2	1	75
3	1.5	85
4	3	82

Reaction conditions: benzaldehyde (281 mg, 1 mmol); ethyltrifluoroacetoacetate (184 mg, 1 mmol); urea (72 mg, 1.2 mmol); PMo11V$SiO_2$1 (10 mg); temperature 80 °C; in solvent-free conditions

[a] The crude product was recrystallized

Table 6 Effect of the amount of catalyst on fluorinated hexahydropyrimidine yields (%)

Entry	Amount of catalyst (mg)	Yield (%)[a]
1	5	81
2	10	85
3	15	86
4	20	86

Reaction conditions: benzaldehyde (281 mg, 1 mmol); ethyltrifluoroacetoacetate (184 mg, 1 mmol); urea (72 mg, 1.2 mmol); PMo11V$SiO_2$1; temperature 80 °C; time, 1.5 h; stirring; in solvent-free conditions

[a] The crude product was recrystallized

Table 7 Catalyst reuse, effect on fluorinated hexahydropyrimidine yields (%)

Entry	Catalytic cycle	Yield (%)[a]
1	1	85
2	2	85
3	3	85
4	4	83

Reaction conditions: benzaldehyde (281 mg, 1 mmol); ethyltrifluoroacetoacetate (184 mg, 1 mmol); urea (72 mg, 1.2 mmol); PMo11V$SiO_2$1 (10 mg); temperature 80 °C; time, 1.5 h, stirring; in solvent-free conditions

[a] The crude product was recrystallized

3.1.5 ^{31}P-MAS-NMR Spectra

The ^{31}P-MAS-NMR spectrum of PMo11 V exhibits a peak at −5.01 ppm assigned to Keggin anion. This signal is present in the silica-included HPA and proves that the Keggin structures are maintained after their inclusion in the silica matrix. As an example, Fig. 4 shows the spectra for PMo11V$SiO_2$2 and PMo11V.

Table 8 Synthesis of fluorinated hexahydropyrimidine

Entry	Product	Yields (%)[a]
1	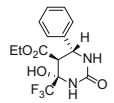	85
2	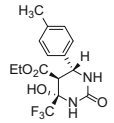	90
3	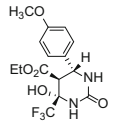	88
4	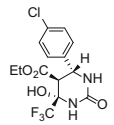	83
5	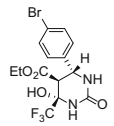	81
6	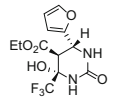	82
7	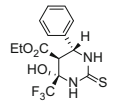	75
8	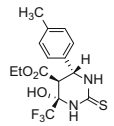	77
9	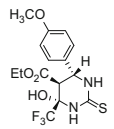	77
10	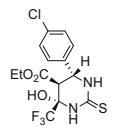	75
11	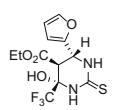	79

Reaction conditions: aldehyde (281 mg, 1 mmol); ethyltrifluoroacetoacetate (184 mg, 1 mmol); urea or thiourea (1.2 mmol); $PMo11VSiO_2$1 (10 mg); temperature 80 °C; 1.5 h; stirring; in solvent-free conditions

[a] The crude product was recrystallized

3.1.6 Potentiometric Titration

Figure 5 shows the potentiometric titration curves for bulk and silica-included HPA. Both bulk HPA, PMo12 and PMo11V are very strong acids (826 and 831 mV, respectively), and they have a high number of acid sites, while the included HPA shows acid sites until 0.5 meq *n*-butylamine. The inclusion of HPA increases the acid strength of silica. It is observed that the initial potential increases with the HPA loading (Table 2).

3.2 Catalytic Test and Suitable Synthesis of Trifluoromethyl Hexahydropyrimidine Derivatives

Optimum reaction conditions were examined employing benzaldehyde, ethyl acetoacetate and urea as test reaction substrates in solvent-free conditions at 80 °C for 1.5 h. In a blank experiment, without the presence of catalyst, only traces (<5 %) of product were detected (Table 3, entry 1). Similarly, a very low reaction yield was obtained when the support (silica sol–gel) was used as catalyst, under the same reaction conditions (Table 3, entry 2, 16 %). Then, the bulk Keggin heteropolyacids PMo12 and PMo11 V were checked under equivalent conditions (Table 3, entries 3 and 4).

In the two experiments, good yields of product 4 were obtained, 48 and 55 %, respectively, indicating that the presence of one acid catalyst in necessary to improve the reaction yields. In previous work we found that the incorporation of V in the structure of PMo increases the number of acidic sites. In this sense, a correlation between the yields and the number of acidic sites was observed [44].

Then, additional tests were carried out with the silica-included catalysts. Four catalysts with different charges were prepared and they were named as: $PMo11VSiO_2$1, $PMo11VSiO_2$2, $PMo11VSiO_2$3, and $PMo11VSiO_2$4. Table 3 (entries 6–9) shows an increase in the reaction yields for the four silica-included catalysts compared to the bulk catalyst. An increase in PMoV loading produces a slight increment in the reaction yields following the sequence: $PMo11VSiO_2$1 (81 %), $PMo11VSiO_2$2 (82 %), $PMo11VSiO_2$3 (84 %), and $PMo11VSiO_2$4 (86 %).

Because the results were similar, and due to the cost of the catalyst, in the next experiment we decided to use the catalyst that has a lower content of active phase ($PMo11VSiO_2$1). The tested experimental reaction conditions were: benzaldehyde (1 mmol); ethyltrifluoroacetoacetate (1 mmol); urea (1.2 mmol); catalyst (5 mg); temperature, 80 °C; time, 1.5 h; stirring; in solvent-free conditions.

We assume that the difference in conversion between bulk and supported catalysts can be explained considering

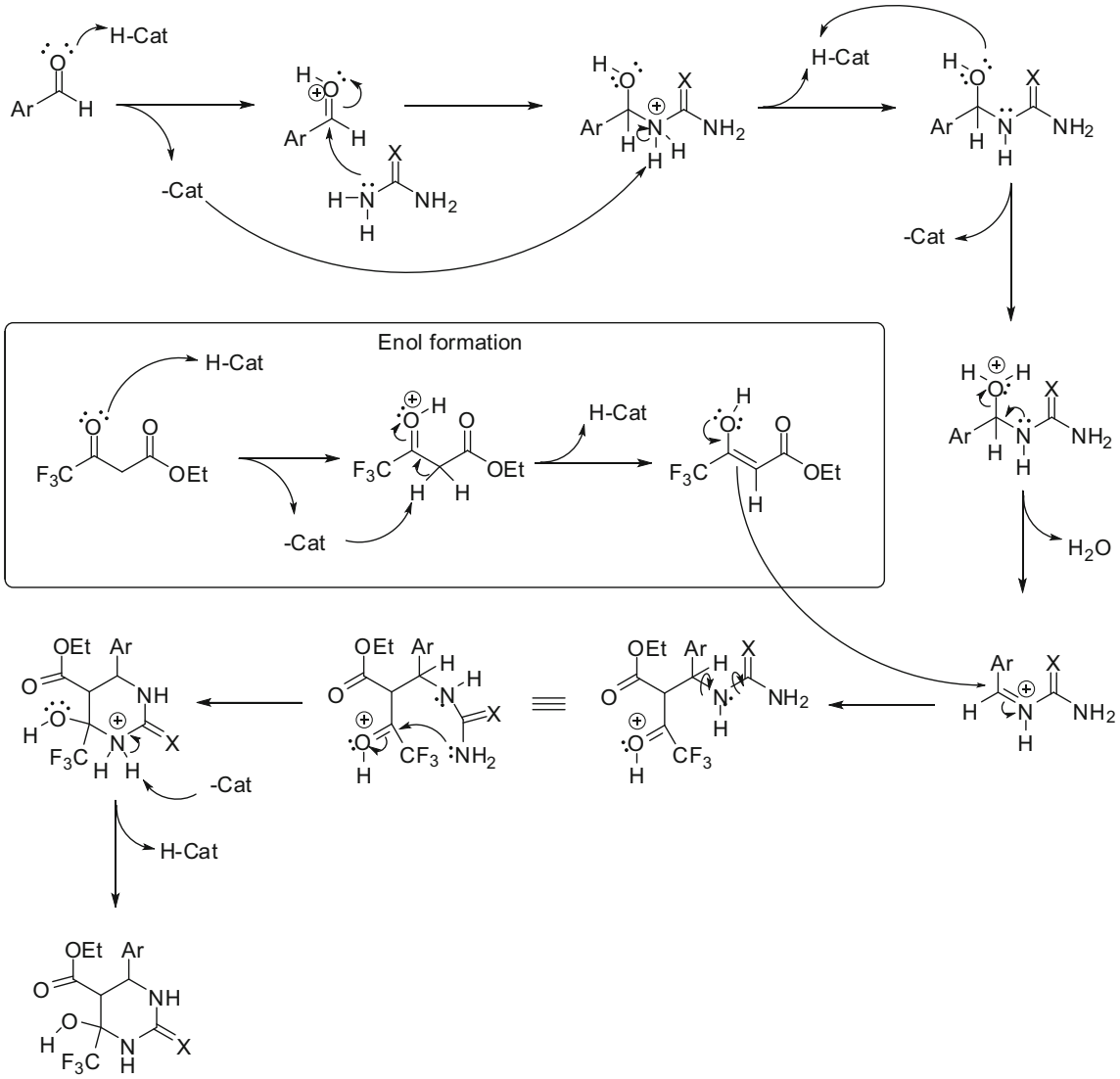

Scheme 2 Plausible reaction mechanism

that they have microporous structure, so the diffusion factor in the whole reaction has a different influence on both systems.

The influence of temperature on the production of the corresponding trifluoromethyl-hexahydropyrimidine is shown in Table 4. Four experiments were performed (25, 60, 80 and 100 °C) working under solvent-free conditions and 1.5 h reaction time at different temperatures. The results show the best yield at 80 ° C (85 %, Table 4, entry 3). The test performed at room temperature (25 °C) gave only a 15 % of reaction product with a low conversion (Table 4, entry 1). Results obtained at 100 °C (Table 4, entry 4, 80 %) show that a temperature higher that 80 °C does not improve the yields. In this case, no unidentified secondary products were detected by TLC. The tested experimental reaction conditions were: benzaldehyde (1 mmol); ethyl 4,4,4-trifluoroacetoacetate (1 mmol); urea (1.2 mmol); catalyst (10 mg); temperature, 80 °C; time, 1.5 h; stirring; in solvent-free conditions.

The reaction time was also tested at the selected optimal temperature of 80 °C, using four different times of 0.5, 1, 1.5 and 3 h (Table 5). A good yield is obtained at 1 h of reaction (Table 5, entry 2, 75 %), reaching the optimal yields at 1.30 h (Table 5, entry 3, 85 %), without any variation at longer reaction times such as 3 h. (Table 5, entry 4, 82 %).

Another key factor in these tests is the amount of the $PMo11VSiO_21$ catalyst. Table 6 shows the results on different proportions of catalyst using the previously defined optimal conditions. It can be seen that 10 mg of $PMo11VSiO_21$ gives very good yields (Table 6, entry 2, 85 %) and no relevant changes were observed when the catalyst increase was 20 mg (Table 6, entry 4, 86 %).

To study the reusability of the catalyst in the same reaction, the recovered catalyst was reused in the same conditions and proportions (80 °C, under solvent-free conditions, with 10 mg of $PMo11VSiO_2$1 and 1:1: 1.2 benzaldehyde: ethyl 4,4,4-trifluoroacetoacetate: urea molar ratio, over four consecutive tests.

To make this possible the recovered catalyst was washed with acetone and dried in vacuum. The results, which are given in Table 7, suggest no appreciable variations when the catalyst is reused four consecutive times.

Based on these results, and using the optimal reaction conditions previously defined (1 mmol of benzaldehyde, 1 mmol of ethyl 4,4,4-trifluoroacetoacetate, 1.2 mmol of urea or thiourea at 80 °C under solvent-free conditions, over a 1.5 h reaction time in the presence of 10 mg of $PMo11VSiO_2$1) different substituted trifluoromethyl hexahydropyrimidines were synthetized. The results listed in Table 8 show very good yields on hexahydropyrimidine derivative formation.

A plausible mechanism is rationalized in Scheme 2. As proposed by Kappe and coworkers [45], the reaction follows a mechanism of acid-catalyzed condensation, in our case with the included heteropolyacid acting as a Bronsted acid catalyst. This reaction begins with protonation of the aldehyde by the acid and is followed by attack, via standard nucleophilic addition, of the urea or thiourea, with some similarities to the Mannich Condensation, to leads *N*-(1-hydroxybenzyl)-ureas or thioureas. Proton transfer steps then result in a protonated alcohol which leaves as water to form a highly reactive *N*-acyliminium species. Then, this intermediate interacts with ethyl acetoacetate enolate to produce an open chain intermediate ureide, which is followed by cyclization to afford the hexahydropyrimidines.

4 Conclusion

In this article, we report the synthesis and characterization of four new Keggin heteropolyacid structures where PMo11V was incorporated in the silica framework by the sol–gel technique. The synthesis of catalysts by the sol–gel technique was satisfactory and the samples kept their HPA structure intact after synthesis. These samples were characterized by ^{31}P-NMR, FT-IR, XRD, and BET. The acidic characteristics of the catalysts were determined by potentiometric titration with *n*-butylamine.

A series of highly substituted hexahydropyrimidines were synthesized using these new materials, encapsulated in a silica framework, as catalyst in solvent-free conditions. This methodology requires short reaction time (1.5 h), a temperature of 80 °C, in solvent-free conditions to obtain good to excellent yields of trifluoromethyl-hexahydropyrimidine derivatives. The Keggin catalyst embedded in the silica matrix is insoluble in polar media, which allows easy removal of the reaction products without affecting their catalytic activity.

The applications of these catalysts in clean oxidation reaction and biomass valorization, are in advance in our laboratory.

Acknowledgments The authors thank CONICET, ANPCyT, UNLP, Centre National de la Recherche Scientifique (CNRS) and the Université Paul Cézanne d'Aix-Marseille for their financial support. VP, AGS, PGV and GPR are members of CONICET.

References

1. Corma A, Garcia H (2006) Adv Synth Catal 348:1391–1412
2. Sheldon R (2012) Chem Soc Rev 41:1437–1451
3. Datan A, Kulkarni A, Torok B (2012) Green Chem 14:17–37
4. Watson W (2012) Green Chem 14:251–256
5. Mulvihill M, Beach M, Zimmerman E, Anastas P (2011) Annu Rev Env Resour 36:271–293
6. Tanaka K (2003) Solvent-free organic synthesis. Willey-VCH, Weinheim
7. Reddy B, Sreekanth P, Lakshmanan P (2005) J Mol Catal A 237:93–100
8. Clark J (2002) Acc Chem Res 35:791–797
9. Okuhara T (2002) Chem Rev 102:3641–3666
10. Misono M, Nojiri N (1990) Appl Catal A 64:1–30
11. Yadav G (2005) Catal Surv Asia 9:117–137
12. Kozhevnikov I (2007) J Mol Catal A 262:86–92
13. Misono M, Ono I, Koyano G, Aoshima A (2002) Pure Appl Chem 72:1305–1311
14. Romanelli G, Sathicq A, Autino J, Thomas H, Baronetti G (2007) Synth Commun 37:3907–3916
15. Sathicq A, Romanelli G, Ponzinibbio A, Baronetti G, Thomas H (2010) Lett Org Chem 7:511–518
16. Ruiz D, Baronetti G, Thomas H, Romanelli G (2012) Curr Catal 1:67–72
17. Pasquale G, Ruiz D, Autino J, Baronetti G, Thomas H, Romanelli G (2012) C. R. Chimie 15:758–763
18. Ruiz D, Autino J, Quaranta N, Vázquez P, Romanelli G (2012) Sci. World J
19. Muñoz M, Sathicq G, Romanelli G, Hernández S, Cabello C, Botto I, Capron M (2013) J Porous Mat 20:65–73
20. Vázquez P, Blanco M, Cáceres C (1999) Catal Lett 60:205–215
21. Caetano C, Fonseca I, Ramos A, Vital J, Castanheiro J (2008) Catal Commun 9:1996–1999
22. Popa A, Sasca V, Kiss E, Marinkovic-Neducin R, Holclajtner-Antunovic I (2011) Mat Res Bull 46:19–25
23. Popa A, Sasca V, Kiss E, Marinkovic-Neducin R, Bokorov M, Holclajtner-Antunovic I (2010) Mat Chem Phys 119:465–470
24. Venkat Rao N, Vaisalini B, Mounika B, Harika L, Kumar Desu V, Nam S (2013) Int J Pharm Chem Res 2:2278–8700
25. Sasada T, Kobayashi F, Sakai N, Konakahara T (2009) Org Lett 11:2161–2164
26. Janati F, Heravi MM, Mirshokraie A (2013) J. Chem
27. Gravier D, Dupin JP, Casadebaig F, Hou G, Boisseau M, Bernard H (1989) Eur J Med Chem 24:531–535
28. Granados R, Alvarez M, Valls N, Salas M (1983) J Heterocycl Chem 20:1271–1275
29. Evans R (1967) Aust J Chem 20:1643–1661
30. Finch H, Peterson E, Ballard S (1952) J Am Chem Soc 8:2016–2018

31. Kappe O, Falsone S, Fabian W, Belaj F (1999) F Heterocycl 51:77–84
32. Saloutin V, Burgart Y, Kuzueva O, Kappe O, Chupakhin O (2000) J Fluor Chem 103:17–23
33. Zohdi H, Rateb N, Elnagdy S (2011) Eur J Med Chem 46:5636–5640
34. Li G, Wu C, Guo L, Yang F (2011) Acta Cryst E67:704–705
35. Bose D, Sudharshan M, Chavhan S (2005) Arkivoc 3:228–236
36. Ryabukhin S, Plaskon A, Ostapchuk E, Volochyuk D, Shishkin O, Tolmachev A (2008) J Fluor Chem 129:625–631
37. Reddy Ch, Mahesh M, Raju P, Babu T, Reddy V (2002) Tetrahedron Lett 43:2657–2659
38. Sathicq Á, Ruiz D, Constantieux T, Rodriguez J, Romanelli G (2014) Synlett 25:881–883
39. Agbaje O, Fadeyi O, Fadeyi S, Myles L, Okoro C, Bioorg C (2011) Med Chem Lett 21:989–992
40. Suresh, Sandhu JS (2012) Arkivoc 1:66–133
41. Kern F, Ruf St, Emig G (1997) Appl Catal A 150:143–151
42. Vázquez P, Pizzio L, Romanelli G, Autino J, Cáceres C, Blanco M (2002) Appl Catal A 235:233–240
43. Martinez JR, Ruiz F (2002) Rev Mex Fis 48:142–149
44. Ďallessandro O, Sathicq G, Palermo V, Sanchez LM, Thomas H, Vázquez P, Constantieux T, Romanelli G (2012) Curr Org Chem 16:2763–2769
45. Kappe CA (1997) J Org Chem 62:7201–7204